energies

MDPI

Article

# High-Performance Accuracy of Daylight-Responsive Dimming Systems with Illuminance by Distant Luminaires for Energy-Saving Buildings

**In-Tae Kim [1], Yu-Sin Kim [1], Meeryoung Cho [1], Hyeonggon Nam [2], Anseop Choi [3] and Taeyon Hwang [2,*]**

[1] Lighting Platform Research Center, Korea Photonics Technology Institute (KOPTI), Gwangju 61007, Korea; itkim@kopti.re.kr (I.-T.K.); yusinkim@kopti.re.kr (Y.-S.K.); cnscmr@kopti.re.kr (M.C.)
[2] School of Architecture, Chosun University, Gwangju 61452, Korea; hyeonggon.nam@chosun.kr
[3] Department of Architectural Engineering, Sejong University, Seoul 05006, Korea; aschoi@sejong.ac.kr
* Correspondence: taeyon.hwang@chosun.ac.kr

Received: 31 December 2018; Accepted: 19 February 2019; Published: 22 February 2019


**Abstract:** In a conventional daylight-responsive dimming system (DRDS), all the luminaires are turned off during the calibration process except for the luminaire under consideration in order to sense only the workplane illuminance of that luminaire. However, the workplane illuminance of the luminaire is influenced by other luminaires. Therefore, the final workplane illuminance of the actual operated system is higher than the target workplane illuminance, reducing the energy-saving efficiency of the DRDS. Herein, to improve the conventional DRDS, an advanced commissioning prediction method of daylight illuminance, and a dimming control algorithm considering the influences by distant luminaires are proposed. To evaluate the accuracy of the proposed prediction method of daylight illuminance, the daylight illuminance on the workplane and the photo sensor values of six points were measured in a full-scale mockup for 27 consecutive days from 22 June to 18 July 2018. As a result of root-mean-square error (RMSE) analysis of daylight illuminance and the photo sensor values, the RMSE (64.86) of P3 located in the middle of the room was the highest, and the RMSE value (17.60) of P5 located near the window was the lowest. In addition, the power consumption of the luminaires, and the target illuminance accuracy of the proposed DRDS were measured and analyzed for 32 consecutive days from 19 July to 19 August 2018 in a full-scale mockup. The average target illuminance accuracy was 96.9% (SD 2.2%), the average lighting energy-savings ratio was 78.4%, and the daylight illuminance prediction accuracy was 95.5% (SD 3.4%).

**Keywords:** LED dimming system; energy savings; daylight; illuminance by distant luminaires

## 1. Introduction

### 1.1. Research Purpose

In 2015, world leaders signed the Paris Climate Convention, which states that greenhouse-gas emissions should be phased out so that the global average temperature does not rise more than 2 °C above pre-industrial levels. Each country must achieve its reduction target in line with the greenhouse-gas emission allowance. To meet this target, the Republic of Korea announced a greenhouse-gas reduction policy. In the construction sector, the Republic of Korea is pursuing a policy of reducing greenhouse-gas emissions through zero-energy buildings. From 2020 onward, public buildings will be obliged to function as zero-energy buildings, and after 2025, private buildings will be obliged to function as zero-energy buildings [1]. Zero-energy buildings require high-efficiency facilities and the active use of renewable energy. Among the various building facilities, lighting installation

constitutes a relatively large proportion (~20%) of the total energy used in buildings [2]. To reduce the energy consumption associated with the installed lighting, light-emitting diode (LED) luminaires are used because they have high efficiency and a long lifetime. Architectural design studies have been performed to reduce the lighting energy consumption by actively using daylight [3–14]. In addition, to further reduce the lighting energy consumption, a daylight-responsive dimming system (DRDS) that utilizes indoor incident daylight is typically used.

In the Republic of Korea, in order to promote LED lighting and to realize zero energy building, more than 32,000 LED luminaires as well as DRDS were installed in Sejong city government office in 2013. The LED luminaire installed at the government office of Sejong city was integrated with a photo sensor, and it was designed so that it could be individually controlled for each luminaire.

The DRDS calculates the workplane illuminance by sensing the incident daylight indoors via a photo sensor installed on the luminaire. If the calculated workplane illuminance exceeds the set target illuminance, the luminaire is turned off, and if the calculated workplane illuminance is less than the target illuminance, the luminaire is dimmed by the difference between the target and calculated workplane illuminance values. In previous studies, the lighting energy savings based on daylight-responsive dimming were in the range of 60%–80% on average [15]. This saving of the lighting energy is a theoretical value that is needed a) to accurately predict the workplane luminance and b) to precisely control dimming. The conventional DRDS (including the DRDS installed in the government office of Sejong city) cannot easily or accurately predict workplane illuminance and does not achieve the theoretical lighting energy savings because it employs a simple dimming control algorithm and a simple commissioning. The simple commissioning is used in the calibration process of the DRDS. The simple commissioning measures the workplane illuminance value at one point only and records the value of the photo sensor in accordance with the dimming level for each luminaire. However, in an actual luminous environment, the illuminance of a particular position is affected by all the luminaires installed in the room. For this reason, the direct learning method is not suitable for the DRDS. Therefore, to improve the energy savings of the DRDS, an advanced commissioning and an advanced dimming control algorithm are proposed. The target illuminance accuracy and the lighting energy savings of the proposed DRDS are analyzed. In this paper, "illuminance by nearest luminaire" represents illuminance by only a specific luminaire to the workplane at a position directly under the luminaire, and "illuminance by distant luminaires" represents illuminance by other than the specific luminaire to the workplane.

### 1.2. State of the Art

Several previous studies have analyzed the accuracy and energy savings of DRDS. Al-Ashwal and Budaiwi (2011) investigated the energy performance of office buildings in hot climates according to the window design. The lighting energy consumption was reduced by 35% through daylight and artificial lighting integration [16]. Fernandes et al. (2013) evaluated the lighting energy savings of a split-pane electrochromic window. The lighting energy savings ranged from 43% to 67% [17]. Caicedo et al. (2014) proposed a control method for achieving target workplane illuminance by using light sensors placed on the ceiling. The proposed method achieved on average 10% less power savings compared with the cases where the light sensors were located at the workspace plane [18]. Yoo et al. (2014) evaluated the LED light energy savings of a DRDS in an office by using light simulation software. The lighting energy savings ranged from 40% to 70% [19]. Gentile and Dubois (2017) investigated the effectiveness of lighting control systems in an office by using simulations based on actual occupancy data. The lighting energy savings ranged from 30% to 55% (in extreme cases) [20]. Nagy et al. (2015) investigated the energy savings of a double-blind occupancy system. The lighting energy savings ranged from 37.9% (compared with the baseline) to 73.2% (compared with a worst-case scenario) [21]. Gentile et al. (2016) performed a monitoring study with four different lighting control systems. The daylight-linked lighting control systems achieved light energy savings of 79% [22].

In a previous study related to lighting control according to occupancy patterns and daylight, Yun et al. (2012) reported field survey results for illuminance distributions, occupancy, and lighting use patterns, as well as the resulting lighting energy demands. There was no significant relationship between the available daylight and the use of lighting by occupants. The lighting use patterns were significantly related to the occupancy patterns [23]. Pandharipande and Caicedo (2011) studied an energy-efficient illumination control design for LED-based lighting systems in office spaces. The results showed that the lighting power savings were in the range of 55% to 57% according to occupancy overlap [24].

Other previously published studies suggested the use of the dimming control algorithm by considering indirect illuminance. Wang and Tan (2013) developed an illumination control method for LED systems based on a neural network model and an energy optimization algorithm by considering the illuminance by distant luminaires. A dimming control algorithm was developed by considering the illuminance by distant luminaires. However, the dimming control algorithm could not be applied to DRDSs, unlike that of our study, which is directly applicable to DRDSs [25]. Choi et al. (2016) proposed the "illuminance by distant luminaires" concept (Method B) for improving the system performance and predicting its lighting energy-saving potential, while inherent problems caused by the open-loop proportional control algorithm were identified. The energy-saving potential of Method B was in the range of 36.9%–73.8% [26]. Similar to the present study, the energy savings were improved by considering the influence of illuminance by distant luminaires. Choi et al. did not apply a DRDS to the test-bed. The energy-saving performance was evaluated through simulations based on the distribution of incident daylight in the condition where all lights were turned off. In the present study, DRDSs were applied to the test-bed. Additionally, the target illuminance accuracy and energy savings were evaluated according to actual measured values. Parise and Martirano (2013) suggested a criterion for evaluating the yearly daylight impact on the energy savings of internal lighting according to the daylight availability, the lighting system layout, and the control system arranged using the daylight lumen method [27]. Ul Haq et al. (2014) reviewed various technologies for lighting control according to the input parameters, controlling methods, control algorithms, cost of installation, complexity of commissioning, etc. The study aimed to investigate the various control system types, the development of the associated technologies, the reported savings from their applications, and the factors that affected their performance [28].

In a previous study related to the prediction of the initial workplane illuminance during daylight, Park et al. (2011) developed an improved closed-loop proportional control algorithm for the DRDS. An improved closed-loop proportional control algorithm was used to predict the varying correlation of photo sensor signals to the daylight workplane illuminance according to the roller shade height and the sky conditions to improve the accuracy of the system [29]. Li et al. (2010) proposed a calculation procedure presented in the form of simple mathematical expressions and diagrams to determine the daylight illuminance on a vertical plane under overcast skies. The performance of the proposed method was evaluated by comparing it with the daylight illuminance simulated using a lighting software (RADIANCE) and with actual sky measurements [30]. Acosta et al. (2015) analyzed the window daylight factors and energy savings in overcast sky conditions. A total of 28 simulations were performed using the lighting simulation program Daylight Visualizer 2.6 and validated via CIE (Comission Internationale de l'Eclairage) test cases [31]. Li (2010) reviewed studies related to daylight illuminance determinations and energy implications because the determinations of the exterior and interior daylight and lighting energy savings were key issues required to demonstrate the benefits of daylighting designs [32].

In summary, previous studies have been implemented to improve or evaluate the energy savings of DRDSs; however, most of them applied the DRDS to simple commissioning or were based on simulation case studies. In this study, the daylight illuminance prediction accuracy, target illuminance accuracy, and real-time power consumption of the DRDS were measured and analyzed by considering the influences of illuminance by distant luminaires in a full-scale mockup.

## 2. Methods

### *2.1. DRDS*

#### 2.1.1. Concept of DRDS

The DRDS uses a photo sensor to calculate the amount of incident daylight (Figure 1). The photo sensor attached to the luminaire measures the amount of incident daylight. According to the measured data, the workplane illuminance is calculated using the slope of the line given by the pre-analyzed workplane illuminance vs. the photo sensor value. To save light energy and maintain the target illuminance, if the calculated workplane illuminance exceeds the set target illuminance, the luminaire is turned off. On the other hand, if the calculated workplane illuminance is less than the target illuminance, the luminaire is dimmed by the difference between the target and calculated workplane illuminance values. First, the photo sensor senses the amount of incident daylight entering into the room while all luminaires are turned off, and predicts the daylight illuminance. When the daylight illuminance is smaller than the target illuminance, the luminaire is turned on, and the difference between the photo sensor values before and after the luminaire turns on. This difference value is calculated as the photo sensor sensing value by solely to luminaire. When the luminous environment is changed by daylight, the calculated photo sensor value by solely to luminaire of the previous stage is subtracted from the current photo sensor value. The current daylight illuminance is predicted by using the subtracted photo sensor value.

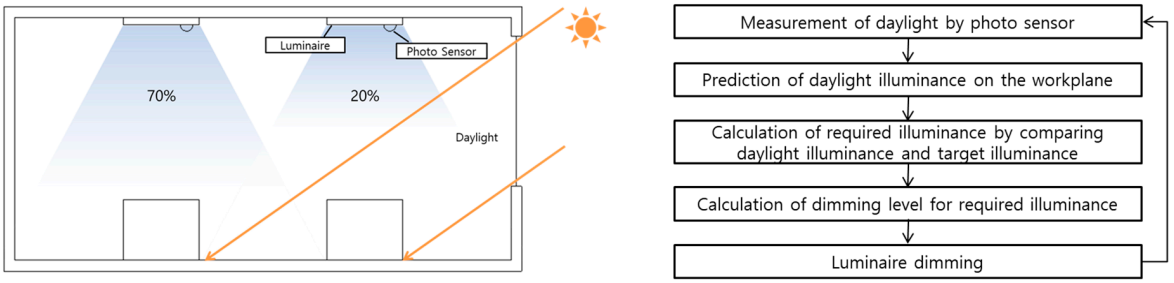


**Figure 1.** Concept of the daylight-responsive dimming system (DRDS).

#### 2.1.2. Prediction Method for Daylight Illuminance on the Workplane

To improve the workplane target illuminance accuracy of the DRDS, it is important to accurately predict the daylight illuminance using the photo sensor attached to the luminaire. To accurately predict the daylight illuminance, it is best to monitor the workplane illuminance in real time by installing an illuminance meter. However, in a practical work environment, an illuminance meter may be obstructed by a worker or a work piece, resulting in a malfunction. Therefore, a method is used for the indirect prediction of the daylight illuminance based on the installation of a photo sensor in the luminaire, which ultimately results in low interference.

To predict the daylight illuminance using the photo sensor installed on the luminaire, the illuminance meter was installed in the workplane environment at a location where daylight is easily detected, as shown in Figure 2. Accordingly, the workplane illuminance and the photo sensor values were measured. The measured data were fitted to regressions and analyzed to calculate the workplane illuminance value regression equation as a function of the sensing value of the photo sensor, as shown in Figure 2. Accordingly, the daylight illuminance prediction algorithm was learnt by the DRDS. When the learning of the daylight illuminance prediction algorithm was completed, the illuminance meter installed was removed, and the workplane illuminance was predicted according to the data sensed by the photo sensor installed on the luminaire. The accuracy of the predicted values of the daylight illuminance increased as the learning process was extended to account for various external environments, seasons, and weather types.

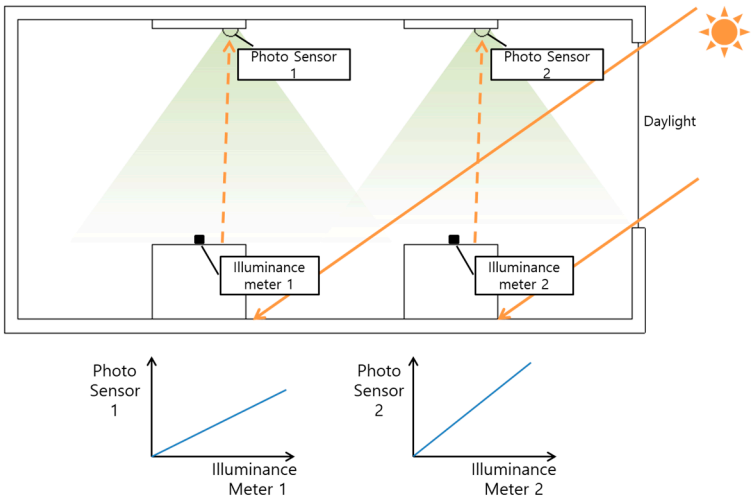


**Figure 2.** Learning method of the daylight illuminance on the workplane prediction algorithm.

### 2.1.3. Simplified Dimming Control Algorithm (Simple Commissioning)

Simple commissioning is used in the calibration process of the DRDS. After sunset, the workplane illuminance and the photo sensor value were measured according to the dimming level of the luminaire. To measure the workplane illuminance, illuminance meters were placed at a position (75 cm above the floor) directly under the luminaires (Figure 3). The workplane illuminance directly under the specific luminaire and the photo sensor value were measured according to the dimming level of the luminaire. When learning about luminaire 1 was implemented, the value of the photo sensor attached to luminaire 1 and the workplane illuminance value directly under luminaire 1 were logged with the dimming level of luminaire 1. During the process of learning about luminaire 1, the value of the photo sensor attached to luminaire 2 and the workplane illuminance value directly under luminaire 2 were not learnt. In this way, during the process of learning about luminaire 2, only the workplane illuminance value directly under luminaire 2 and the value of the photo sensor attached to luminaire 2 were learnt.

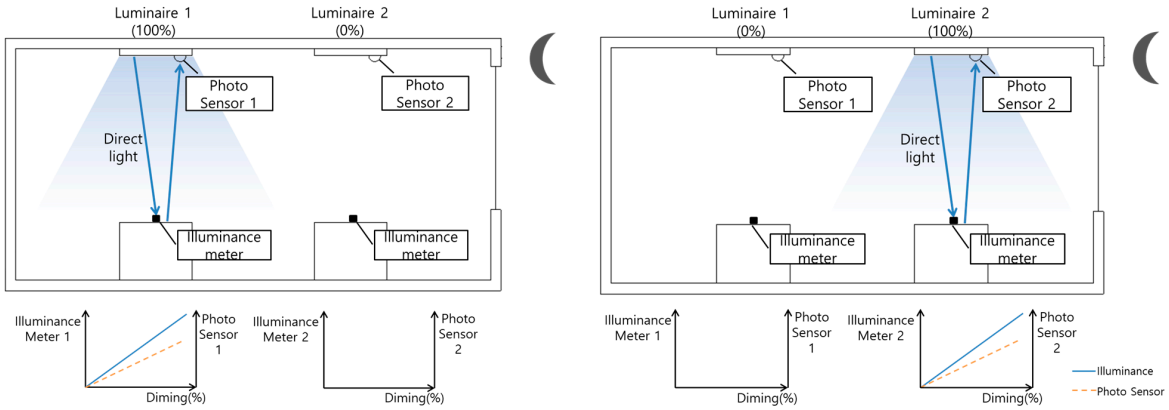


**Figure 3.** System processes of simple commissioning: (**a**) learning process for luminaire 1; (**b**) learning process for luminaire 2.

The simple commissioning was relatively easy, and it was possible to learn in a short time. However, in the actual luminous environment, the workplane illuminance directly under luminaire 1 was influenced by distant luminaires from luminaire 2. Therefore, the final workplane illuminance of the actual operated system was higher than the target workplane illuminance (Figure 4). This reduces the energy-saving efficiency of the DRDS.

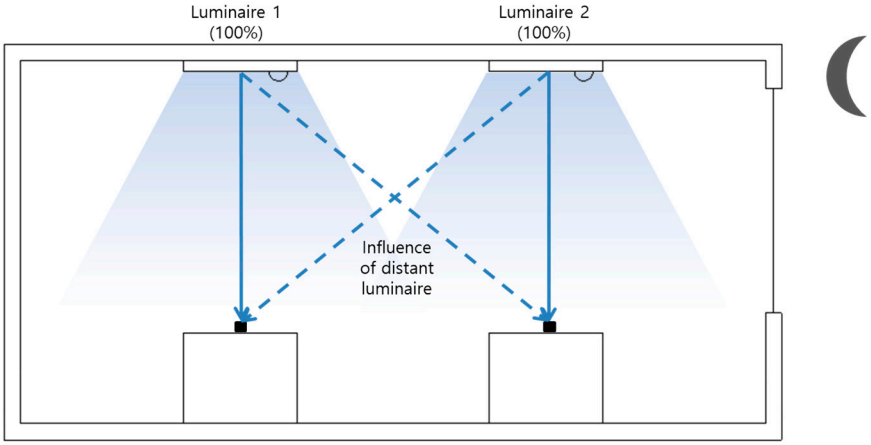


**Figure 4.** Actual luminous environments affected by the nearest and the distant luminaire.

If the photo sensor detected that the workplane illuminance value exceeded the target workplane illuminance value, the luminaires were dimmed by a value equal to the difference between the target and the actual illuminances. The luminaires were excessively dimmed because the simple commissioning algorithm does not consider illuminance by distant luminaires. To maintain the target illuminance, the DRDS applied the simple commissioning repeatedly with illumination and over-dimming (Figure 5a). If the illuminance by the distant luminaires component was larger than the illuminance by the nearest luminaire component, the final workplane illuminance diverged, and the target illuminance could not be maintained (Figure 5b).

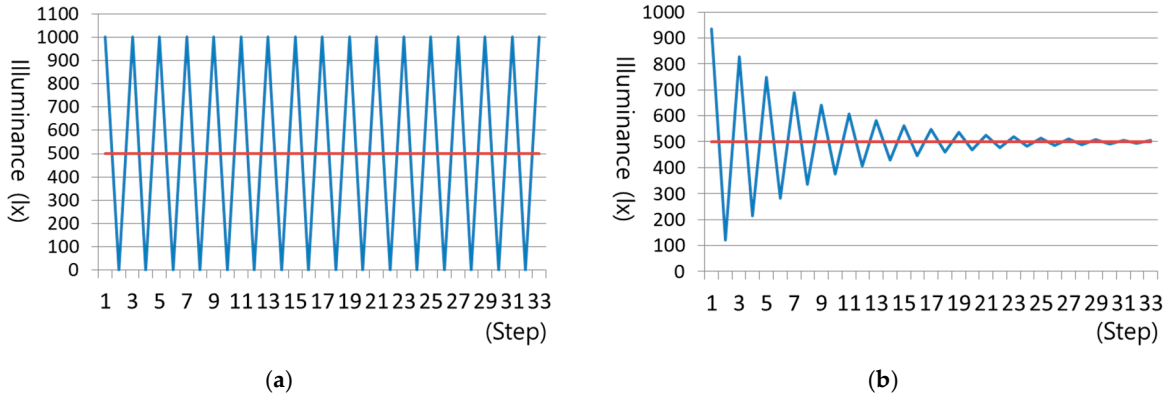


**Figure 5.** Maintaining the target illuminance of the DRDS with application of simple commissioning: (**a**) convergence case; (**b**) divergence case.

### 2.1.4. Proposed Dimming Control Algorithm (Advanced Commissioning)

To improve the accuracy and energy savings of the conventional DRDS, an advanced commissioning and a dimming control algorithm considering the influences of illuminance by distant luminaires were proposed. In contrast to the simple commissioning, the workplane illuminances of all the points and the photo sensor values of all the luminaires were logged according to the dimming level of each luminaire (Figure 6).

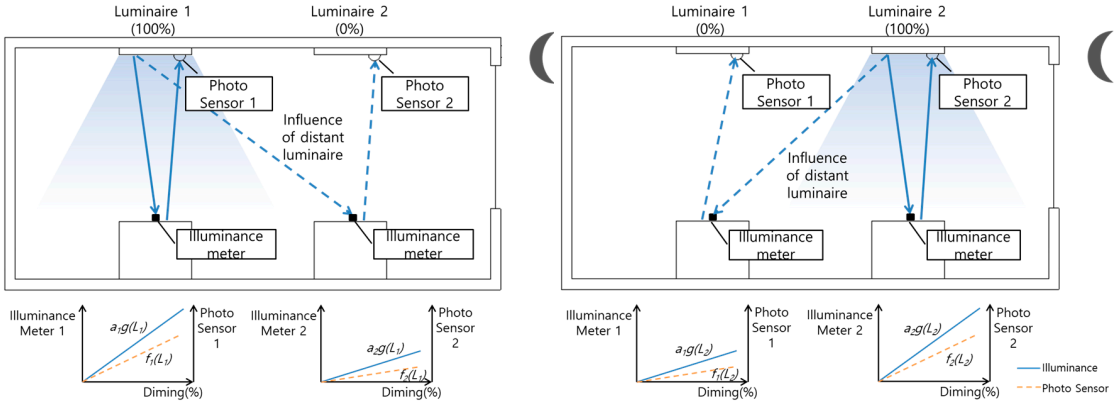


**Figure 6.** System processes of advanced commissioning: (**a**) learning process for luminaire 1; (**b**) learning process for luminaire 2.

Assuming that daylight enters a room with six luminaires, as shown in Figure 7, the final workplane illuminance ($ET_1$) at the position directly under luminaire 1 can be calculated using Equation (1). The final workplane illuminance is the sum of the daylight illuminance, illuminance by the nearest luminaire, and illuminance by distant luminaires. The final workplane illuminance ($ET_j$) of all the points can be calculated using the standardized Equation (2).

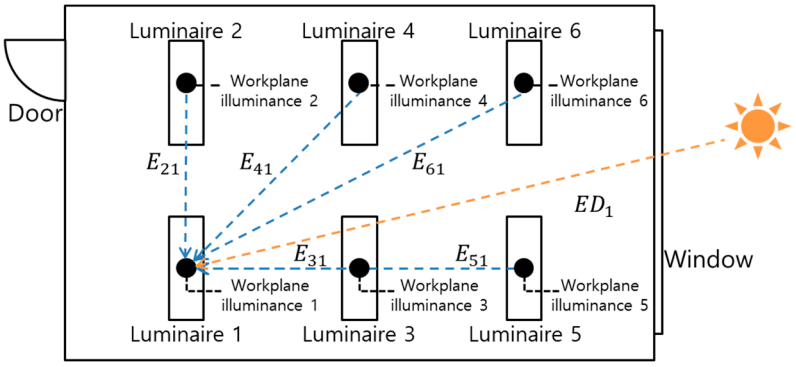


**Figure 7.** Calculation methods for illuminance by the nearest luminaire and the distant luminaires.

$$ET_1 = ED_1 + E_{11} + E_{21} + E_{31} + E_{41} + E_{51} + E_{61} \quad (1)$$

$ED_1$ = Daylight illuminance at the position directly under luminaire (1)
$E_{ij}$ = Workplane illuminance at the position directly under luminaire (j) from luminaire (i)

$$ET_j = ED_j + \sum_{i=1}^{n} E_{ij} \quad (2)$$

$ET_j$ = Final workplane illuminance at the position directly under luminaire (j)
$ED_j$ = Daylight illuminance at the position directly under luminaire (j)
$n$ = Number of luminaires

In the case where the target workplane illuminance is set as 500 lx, if $ED_1$ is 200 lx, the required workplane illuminance at workplane illuminance 1 ($ER_1$) can be calculated using Equation (3). The required illuminance at the position directly under luminaire (j) ($ER_j$) can be defined using Equation (3), according to Equation (4).

$$\sum_{i=1}^{6} E_{i1} = ET_1 - ED_1 = 500lx - 200lx = 300lx = ER_1 \quad (3)$$

$$\begin{aligned} E_{11} + E_{21} + E_{31} + E_{41} + E_{51} + E_{61} &= ER_1 \\ E_{12} + E_{22} + E_{32} + E_{42} + E_{52} + E_{62} &= ER_2 \\ E_{13} + E_{23} + E_{33} + E_{43} + E_{53} + E_{63} &= ER_3 \\ E_{14} + E_{24} + E_{34} + E_{44} + E_{54} + E_{64} &= ER_4 \\ E_{15} + E_{25} + E_{35} + E_{45} + E_{55} + E_{65} &= ER_5 \\ E_{16} + E_{26} + E_{36} + E_{46} + E_{56} + E_{66} &= ER_6 \end{aligned} \tag{4}$$

If the regression equations of the workplane illuminances according to the dimming level with the use of the advanced commissioning are defined according to Equation (5), Equation (4) can be used to define the simultaneous set of linear equations with six variables, as indicated by Equation (6).

$$\begin{aligned} &E_{ij} = IE_{ij}\, g(L_j) \\ &g(L_j) = \text{Regression equation of the workplane illuminance at the position directly under luminaire (j) according to the dimming level of luminaire (j)} \\ &IE_{ij} = \text{Proportion of the workplane illuminance at the position directly under luminaire (i) and the workplane illuminance at the position directly under luminaire (j) by luminaire (i)} \end{aligned} \tag{5}$$

$$\begin{aligned} IE_{11}g(L_1) + IE_{21}g(L_2) + IE_{31}g(L_3) + IE_{41}g(L_4) + IE_{51}g(L_5) + IE_{61}g(L_6) &= ER_1 \\ IE_{12}g(L_1) + IE_{22}g(L_2) + IE_{32}g(L_3) + IE_{42}g(L_4) + IE_{52}g(L_5) + IE_{62}g(L_6) &= ER_2 \\ IE_{13}g(L_1) + IE_{23}g(L_2) + IE_{33}g(L_3) + IE_{43}g(L_4) + IE_{53}g(L_5) + IE_{63}g(L_6) &= ER_3 \\ IE_{14}g(L_1) + IE_{24}g(L_2) + IE_{34}g(L_3) + IE_{44}g(L_4) + IE_{54}g(L_5) + IE_{64}g(L_6) &= ER_4 \\ IE_{15}g(L_1) + IE_{25}g(L_2) + IE_{35}g(L_3) + IE_{45}g(L_4) + IE_{55}g(L_5) + IE_{65}g(L_6) &= ER_5 \\ IE_{16}g(L_1) + IE_{26}g(L_2) + IE_{36}g(L_3) + IE_{46}g(L_4) + IE_{56}g(L_5) + IE_{66}g(L_6) &= ER_6 \end{aligned} \tag{6}$$

Equation (7) is transformed by Equation (6). To calculate $g(L_j)$, the inverse proportion of the workplane illuminance matrix of Equation (7) is transformed into Equation (8). The dimming level that satisfies the required illuminance value of each point can be calculated using the calculated $g(L_j)$.

$$\begin{pmatrix} IE_{11} & IE_{21} & IE_{31} & IE_{41} & IE_{51} & IE_{61} \\ IE_{12} & IE_{22} & IE_{32} & IE_{42} & IE_{52} & IE_{62} \\ IE_{13} & IE_{23} & IE_{33} & IE_{43} & IE_{53} & IE_{63} \\ IE_{14} & IE_{24} & IE_{34} & IE_{44} & IE_{54} & IE_{64} \\ IE_{15} & IE_{25} & IE_{35} & IE_{45} & IE_{55} & IE_{65} \\ IE_{16} & IE_{26} & IE_{36} & IE_{46} & IE_{56} & IE_{66} \end{pmatrix} \begin{pmatrix} g(L_1) \\ g(L_2) \\ g(L_3) \\ g(L_4) \\ g(L_5) \\ g(L_6) \end{pmatrix} = \begin{pmatrix} ER_1 \\ ER_2 \\ ER_3 \\ ER_4 \\ ER_5 \\ ER_6 \end{pmatrix} \tag{7}$$

$$\begin{pmatrix} g(L_1) \\ g(L_2) \\ g(L_3) \\ g(L_4) \\ g(L_5) \\ g(L_6) \end{pmatrix} = \begin{pmatrix} IE_{11} & IE_{21} & IE_{31} & IE_{41} & IE_{51} & IE_{61} \\ IE_{12} & IE_{22} & IE_{32} & IE_{42} & IE_{52} & IE_{62} \\ IE_{13} & IE_{23} & IE_{33} & IE_{43} & IE_{53} & IE_{63} \\ IE_{14} & IE_{24} & IE_{34} & IE_{44} & IE_{54} & IE_{64} \\ IE_{15} & IE_{25} & IE_{35} & IE_{45} & IE_{55} & IE_{65} \\ IE_{16} & IE_{26} & IE_{36} & IE_{46} & IE_{56} & IE_{66} \end{pmatrix}^{-1} \begin{pmatrix} ER_1 \\ ER_2 \\ ER_3 \\ ER_4 \\ ER_5 \\ ER_6 \end{pmatrix} \tag{8}$$

### *2.2. Evaluation*

In order to verify the performance of the DRDS proposed in this study, a demonstration evaluation was conducted on a full scale mock-up test-bed. The demonstration evaluation was divided into the evaluation preparation stage and the evaluation stage as shown in Figure 8. In the evaluation preparation stage, advanced commissioning was performed, and the prediction algorithm for the daylight illuminance was developed through the preliminary measurement of the daylight illuminance and photo sensor values for 27 days. In the evaluation stage, the demonstration evaluation of the proposed DRDS was conducted. The measuring elements were workplane illuminance, daylight illuminance, photo sensor value, lighting power consumption, and external horizontal solar radiation.

Based on the measured results, the target illuminance accuracy, daylight illuminance prediction accuracy, and lighting energy savings of the proposed DRDS were analyzed.

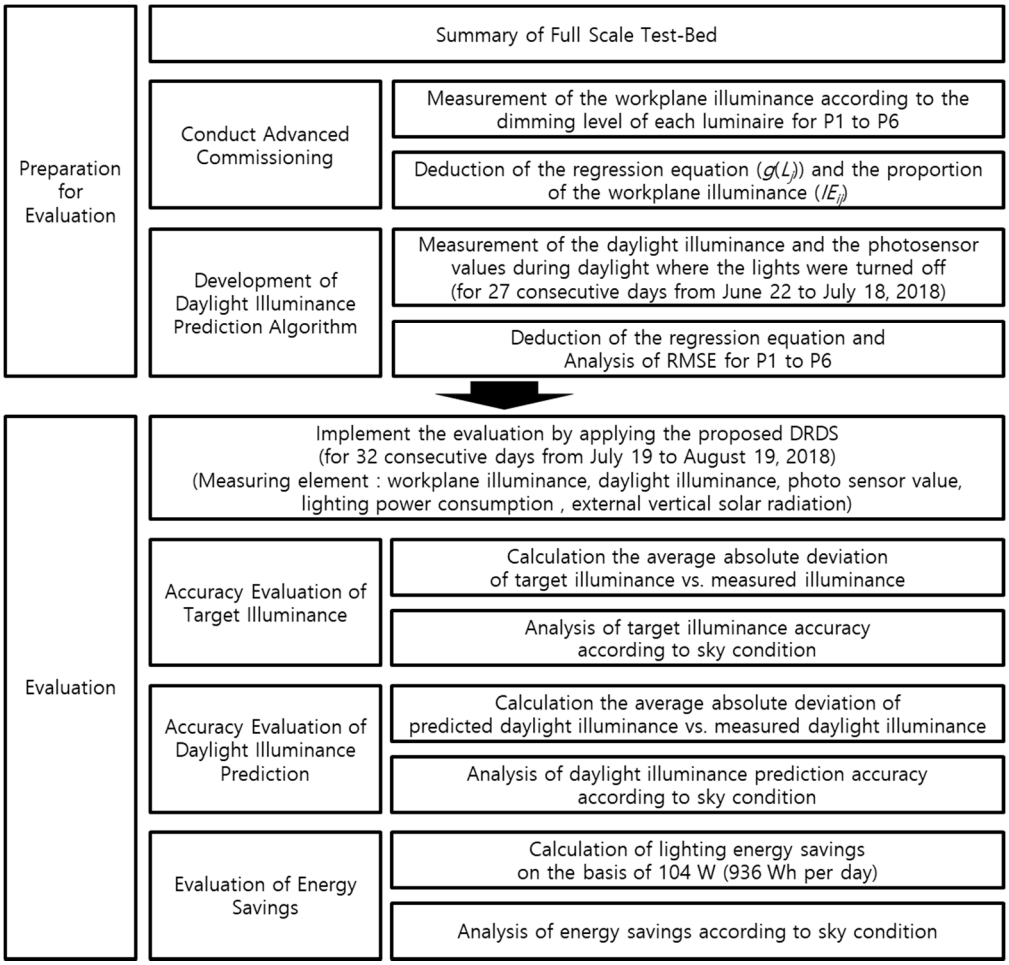


**Figure 8.** Flow chart of evaluation.

### 2.2.1. Test-Bed

The accuracy of the daylight illuminance on the workplane prediction, the energy savings, and the accuracy of the target workplane illuminance of the proposed DRDS were evaluated. The evaluation was implemented using a full-scale test-bed (Figure 9). The size of the test-bed was 2750 (W) × 6000 (L) × 2700 (H) (mm). Six luminaires (LED, 1200 × 300 mm$^2$, 40 W, built-in photo sensor) were installed in the test-bed. The test-bed was located in the Gwangju metropolitan city in the Republic of Korea. The azimuth angle of the test-bed was 23° (SW). To measure workplane illuminance, illuminance meters (P1–P6) were placed at the workplane height (750 mm) under each luminaire.


**Figure 9.** Outline of the full-scale test-bed.

Before evaluation, a calibration process was performed using advanced commissioning. The regression equation ($g(L_j)$) of the workplane illuminance at the position under luminaire (j) was analyzed according to the dimming level of luminaire (j) (Figure 10 and Table 1). The luminaire dimming was adjustable in 20 steps (5% increments per step). Additionally, the proportion of the workplane illuminance ($IE_{ij}$) at the position directly under luminaire (i) and the workplane illuminance at the position directly under luminaire (j) were analyzed, as shown in Table 2. The maximum illuminance values of $g(L_1)$ and $g(L_2)$ near the window were measured to be approximately 400 lx. In comparison, the maximum illuminance values of $g(L_3)$, $g(L_4)$, $g(L_5)$, and $g(L_6)$ near the door and middle areas were measured to be approximately 500 lx. It was considered that $g(L_1)$ and $g(L_2)$ had low-illuminance values because the window transmitted artificial light outside without reflecting it.

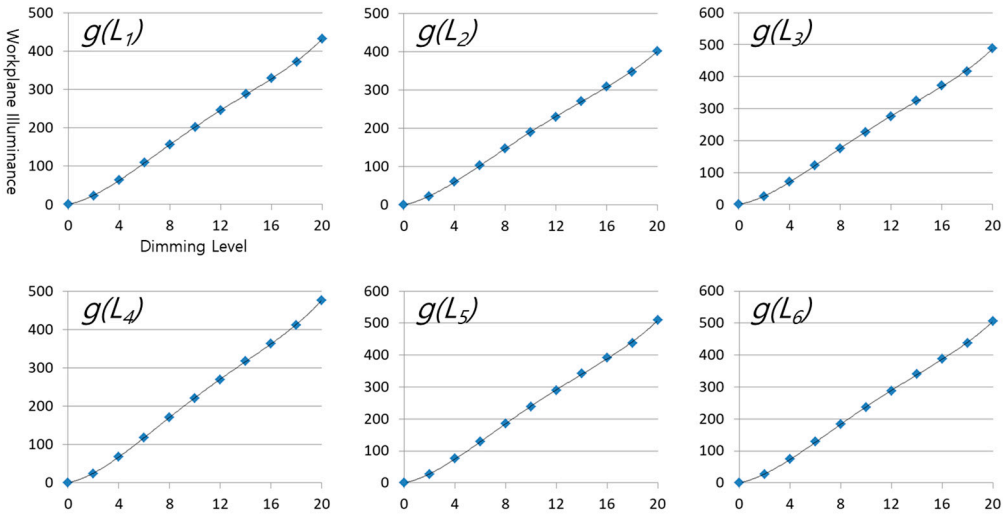


**Figure 10.** Workplane illuminance according to the dimming levels.

**Table 1.** Regression equations of $g(L_j)$ of the dimming level illuminance at the workplane.

| | $x^4$ | $x^3$ | $x^2$ | x | Adjusted $R^2$ |
|---|---|---|---|---|---|
| $g(L_1)$ | 0.0051 | −0.2112 | 2.9129 | 7.1438 | 0.9999 |
| $g(L_2)$ | 0.0045 | −0.1894 | 2.6403 | 7.0639 | 0.9999 |
| $g(L_3)$ | 0.006 | −0.251 | 3.4595 | 7.2117 | 0.9999 |
| $g(L_4)$ | 0.0055 | −0.2328 | 3.2959 | 7.0318 | 0.9999 |
| $g(L_5)$ | 0.006 | −0.2531 | 3.5007 | 8.2746 | 0.9999 |
| $g(L_6)$ | 0.0058 | −0.2436 | 3.413 | 8.2883 | 0.9999 |

**Table 2.** Proportion of workplane illuminance by distant luminaires ($IE_{ij}$).

| | P1 (j = 1) | P2 (j = 2) | P3 (j = 3) | P4 (j = 4) | P5 (j = 5) | P6 (j = 6) |
|---|---|---|---|---|---|---|
| $L_1$ (i = 1) | 1 | 0.557 | 0.356 | 0.269 | 0.095 | 0.092 |
| $L_2$ (i = 2) | 0.470 | 1 | 0.245 | 0.372 | 0.085 | 0.099 |
| $L_3$ (i = 3) | 0.361 | 0.264 | 1 | 0.558 | 0.339 | 0.257 |
| $L_4$ (i = 4) | 0.247 | 0.372 | 0.471 | 1 | 0.222 | 0.338 |
| $L_5$ (i = 5) | 0.094 | 0.086 | 0.362 | 0.273 | 1 | 0.567 |
| $L_6$ (i = 6) | 0.092 | 0.100 | 0.267 | 0.379 | 0.510 | 1 |

### 2.2.2. Prediction Algorithm of Daylight Illuminance on the Workplane

To develop the daylight illuminance on the workplane prediction algorithm before the evaluation of the accuracy and energy savings, the daylight illuminance and the photo sensor values were measured simultaneously during daylight for the prediction of the daylight illuminance in a room where the lights were turned off. The measurements were conducted for 27 consecutive days from

22 June to 18 July 2018. A regression analysis was performed for each of the measured values at each measurement point (P1–P6) to derive a regression equation (Figure 11 and Table 3). Assuming that the office could be used as the test-bed, the target illuminance was set to 500 lx (Korean standard, KS-illuminance standard) [33]. Therefore, if the daylight illuminance exceeded 500 lx, it was excluded from the regression analyses.

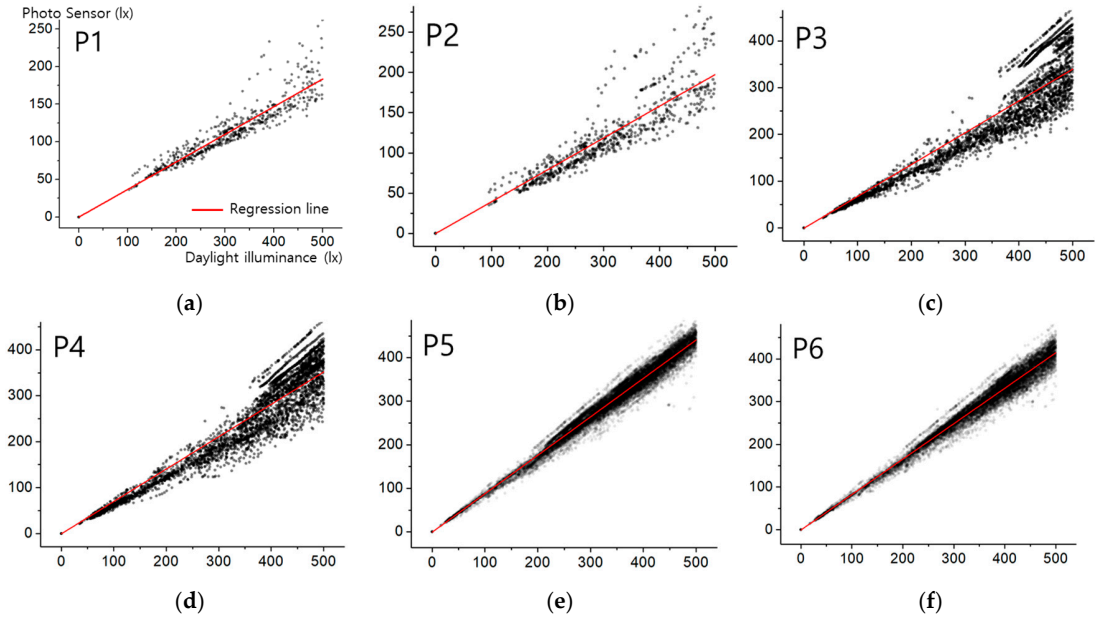


**Figure 11.** Results of regression analyses (photo sensor value vs. daylight illuminance) for (**a**) P1, (**b**) P2, (**c**) P3, (**d**) P4, (**e**) P5, and (**f**) P6.

**Table 3.** Gradients of regression lines (photo sensor value vs. daylight illuminance).

| | P1 | P2 | P3 | P4 | P5 | P6 |
|---|---|---|---|---|---|---|
| Gradient | 0.3669 | 0.3950 | 0.6797 | 0.7040 | 0.8827 | 0.8295 |
| Adjusted $R^2$ | 0.9695 * | 0.9844 | 0.9698 | 0.9804 | 0.9976 ** | 0.9970 |
| RMSE | 40.89 | 57.23 | 64.86 ** | 52.22 | 17.60 * | 20.00 |

* Minimum value, ** Maximum value. RMSE = root-mean-square error

The adjusted coefficient of determination ($R^2$) was close to unity and exhibited a distinct trend. The regression analyses showed that the adjusted coefficient of determination (0.9695) of P1 located in the middle of the room was the lowest, and the adjusted coefficient of determination (0.9976) of P5 located near the door was the highest. Classification and comparison of the results according to areas showed that the adjusted coefficient of determination values at the door, window, and middle areas were high.

The fact that the root-mean-square error (RMSE) value is close to zero indicates that the error between the predicted model and the measured value was small. RMSE analyses showed that the RMSE value (64.86) of P3 located in the middle of the room was the highest, and the RMSE value (17.60) of P5 located near the window was the lowest. Comparison of the results by area indicated that the RMSE values of the door, window, and middle areas were low. Near the window, most of the daylight illuminance values exceeded 500 lx during daylight. When the workplane illuminance value did not exceed 500 lx, the sky condition was classified as overcast, or there was no direct incident sunlight. For this reason, the deviation in the window area was smaller than the deviation in the middle area. Conversely, in the middle area, there were many cases where the daylight illuminance values were <500 lx despite direct incident sunlight. Therefore, it was considered that the deviation in the middle area was greatly affected by the depth and angle of the direct sunlight. It was considered that the door area had the smallest deviation because it was influenced by diffused light more than direct sunlight, regardless of the incident direct sunlight.

## 3. Results

### *3.1. Evaluation of Target Illuminance Accuracy*

In this study, the target illuminance accuracy of the DRDS, which used the proposed dimming control algorithm, was evaluated. The daylight illuminance was predicted when all the luminaires were turned off (Figure 12). The inverse value of the analyzed gradient of Table 2 was applied to the DRDS. The daylight illuminance was predicted by multiplying the measured values from the photo sensor by the inverse value of the gradient. The required dimming level was calculated by inputting the predicted daylight illuminance to the proposed dimming control algorithm (Step 1). To evaluate the daylight illuminance prediction accuracy, the daylight illuminance was logged in Step 1. All the luminaires were automatically dimmed according to the calculated required dimming level values. After dimming, the final workplane illuminance that combined artificial light and daylight was measured. Additionally, the power consumption of the luminaires was measured (Step 2).

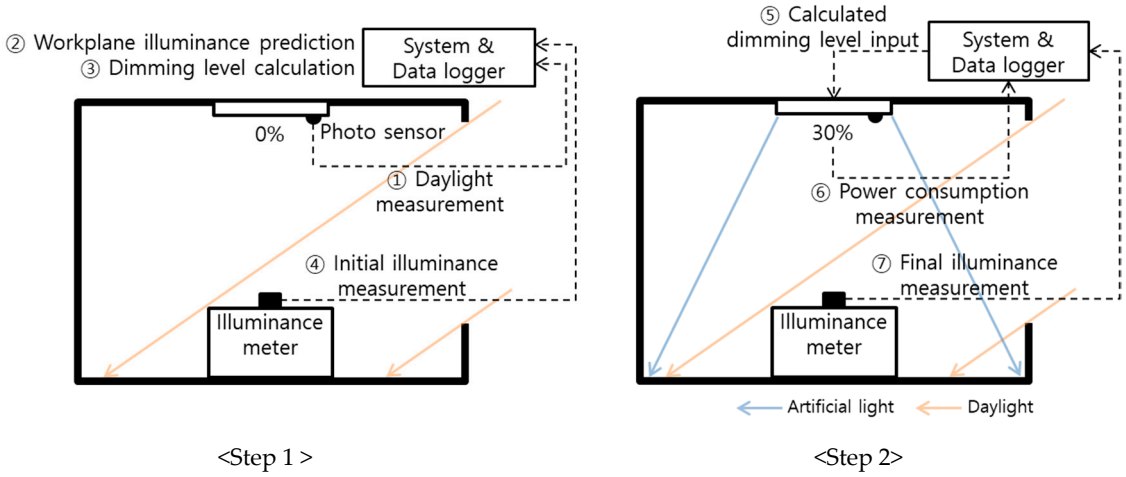


**Figure 12.** Process of evaluating the target illuminance accuracy, daylight illuminance on workplane prediction accuracy, and energy savings.

The target illuminance accuracy and daylight illuminance prediction accuracy were evaluated for 32 consecutive days from 19 July to 19 August 2018. The daily measurements were conducted at 1-min intervals from 9:00 am to 6:00 pm. The summer season in the Republic of Korea extends from June to September. During the summer—with the exception of the rainy season—there is plenty of sunshine for long durations.

The target illuminance accuracy was evaluated by comparing the measured final workplane illuminance and the target illuminance for all measurement points. When the daylight illuminance exceeded the target illuminance, it was excluded from the evaluation. For instance, when the daylight illuminance of P1 and P2 exceeded the target illuminance, P3 to P6 were evaluated, rather than P1 and P2. Also, the average target illuminance accuracy was calculated by calculating the average absolute deviation. Figure 13 shows the daily measurements results for the final workplane illuminance obtained with the proposed DRDS from 19 July to 19 August 2018. The analyzed results for the target illuminance accuracy are shown in Figure 14.

As shown in Figure 13, the final workplane illuminances of P1 and P2 placed near the window were almost higher than the target illuminance (500 lx). Therefore, luminaires 1 and 2 were nearly turned off, showing the maximum energy-saving efficiency. Conversely, the final workplane illuminances of points P5 and P6 near the door were almost 500 lx. Accordingly, the illuminance was kept constant at the target illuminance (500 lx) by the proposed DRDS. Figure 14 shows the daily target illuminance accuracy results for the target illuminance. The daily target illuminance accuracy was calculated within the average of the accuracy of all the measurement points during the

day. The total average target illuminance accuracy was high (96.9%, SD 2.2%). The maximum and minimum accuracies were 100% and 73.9%, respectively.

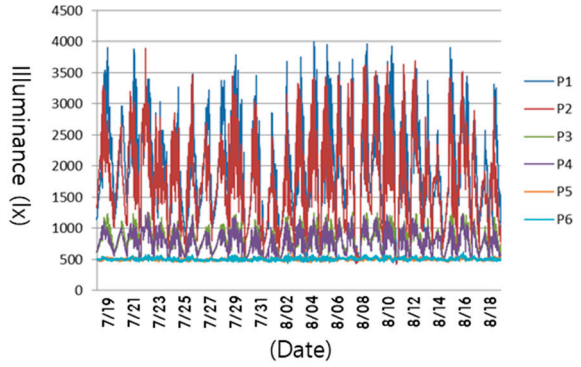


**Figure 13.** Daily measurement results for the final workplane illuminance.

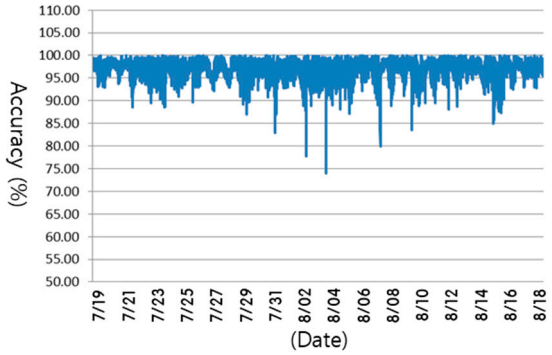


**Figure 14.** Daily accuracy results for the target illuminance.

In order to compare and analyze the result data according to the sky condition, the horizontal solar radiation value was measured through the solar radiation sensor installed on the test bed roof. The clearness index ($K_T$) was calculated using the measured the horizontal solar radiation value. Clearness index is the ratio of the global solar radiation measured at the surface to the total solar radiation at the top of the atmosphere [34]. If the clear index is 1, it can be seen that there is no cloud in the sky. Also, if the clear index approaches 0, it can be seen that the sky is completely covered with clouds.

The results of the comparison analyses of the target illuminance accuracy and the clearness index are shown in Figure 15. Regression analysis of the target illuminance accuracy data and the clear index data showed that the coefficient of determination ($R^2$) value was 0.0087. The coefficient of determination is the proportion of the variance in the dependent variable that is predictable from the independent variable. If the coefficient of determination is close to 1 it indicates that the trend between the accuracy and clearness index was similar. As a regression analysis results, there is no correlation between the target illuminance accuracy data and the clear index data.

Table 4 shows the average target illuminance accuracies at points P1–P6 according to the sky conditions. Clearness index values of 0.75 or higher correspond to clear skies. When the clearness index was between 0.25 and 0.75, the sky was partly cloudy. A clearness index of <0.25 corresponds to an overcast sky [35,36]. The P1 and P2 values for partly cloudy skies in Table 3 were excluded from the accuracy calculation because the daylight illuminances of P1 and P2 during daylight exceeded the target illuminance value. In the case of clear skies, the average target illuminance accuracy values of P1 and P2 were calculated according to 4–5 valid measured datasets (approximately 2,000 datasets in total). Therefore, the values were not reliable. All the measured points (P1–P6) yielded higher accuracy values for overcast skies than for clear skies.

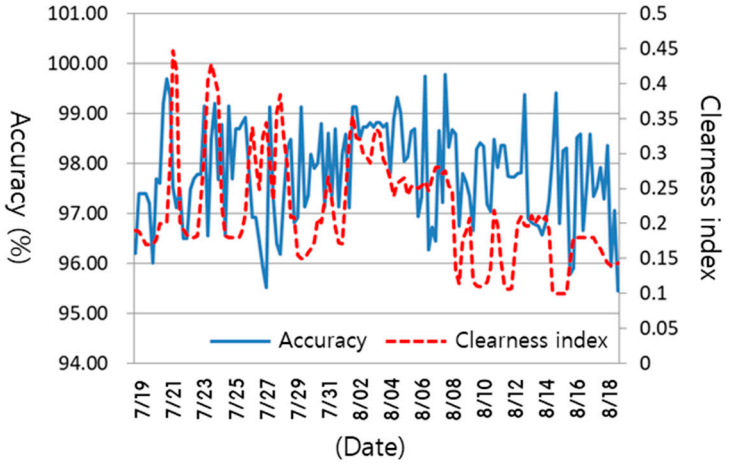


**Figure 15.** Variations of the target illuminance accuracy and clearness index.

**Table 4.** Average target illuminance accuracies at points P1–P6 according to the sky conditions.

| Sky Condition | P1 (%) | P2 (%) | P3 (%) | P4 (%) | P5 (%) | P6 (%) |
|---|---|---|---|---|---|---|
| Clear | 91.41 | 87.72 | 87.07 * | 89.49 | 96.13 ** | 94.27 |
| Partly cloudy | - | - | 83.85 * | 89.55 | 97.13 ** | 97.00 |
| Overcast | 96.39 | 95.71 | 93.62 * | 94.11 | 97.15 | 97.18 ** |

* Minimum value, ** Maximum value.

### 3.2. Evaluation of Daylight Illuminance Prediction Accuracy

The daylight illuminance prediction accuracy was calculated by comparing the predicted and measured daylight illuminances. The data for which the measured daylight illuminance exceeded the target illuminance were excluded from the prediction accuracy calculation. Figure 16 shows the prediction accuracy results for the daylight illuminance. The average daylight illuminance prediction accuracy was 95.5% (SD 3.4%). The maximum accuracy was 100%, and the minimum accuracy was 71.46%.

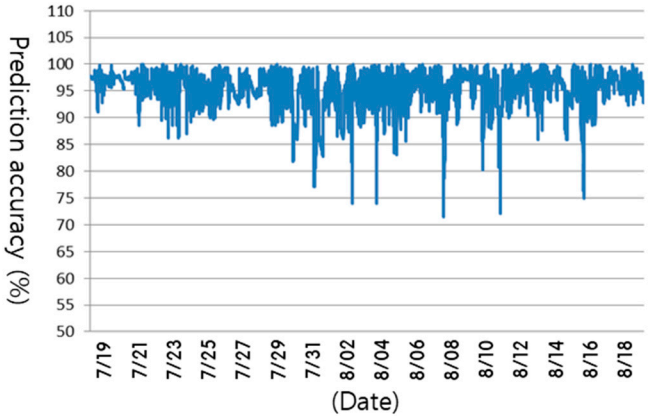


**Figure 16.** Daily results for the daylight illuminance on the workplane prediction accuracy.

Table 5 shows the average, maximum, minimum, standard deviation, and RMSE values of the daylight illuminance prediction accuracy at various points. The RMSE value is the root-mean-square error and close to zero indicates that the error between the predicted model and the measured value was small. Figure 17 shows the scatter plots of the predicted and measured values of the daylight illuminance for each studied point. The closeness of the points of the scatter plot to the 1:1 regression line indicates the closeness of the predicted and measured values. The trend of the RMSE values in Table 5 is similar to the trend of the RMSE values (daylight illuminance–photo sensor values) in

Table 2. As the variance of the scatter data of the daylight illuminance–photo sensor values increased, the prediction accuracy of the daylight illuminance decreased.

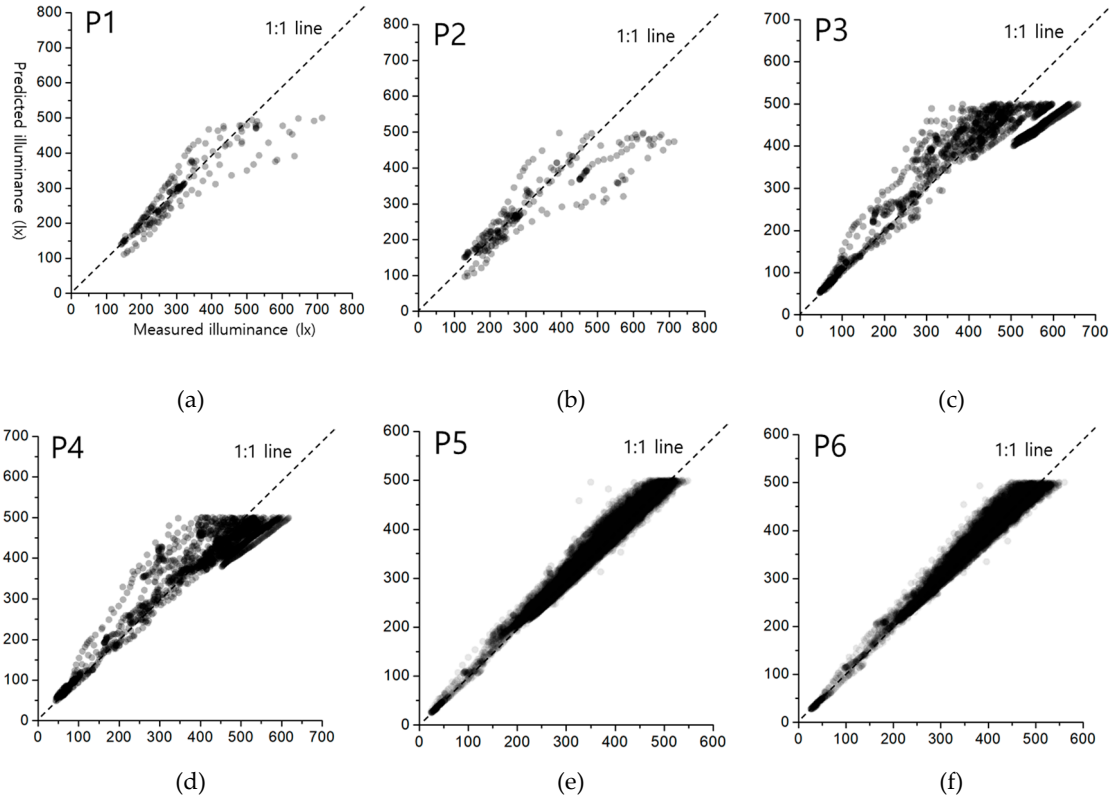


**Figure 17.** Prediction accuracy of the daylight illuminance on the workplane at points (**a**) P1, (**b**) P2, (**c**) P3, (**d**) P4, (**e**) P5, and (**f**) P6.

**Table 5.** Accuracy analysis for the prediction of the daylight illuminance on the workplane at points P1–P6.

| | P1 | P2 | P3 | P4 | P5 | P6 |
|---|---|---|---|---|---|---|
| Average (%) | 88.99 | 84.25 * | 86.41 | 89.39 | 95.99 | 96.00 ** |
| SD (%) | 11.58 | 15.44 ** | 9.93 | 7.37 | 3.07 * | 3.15 |
| Max (%) | 99.96 | 99.86 | 99.93 | 99.99 | 100.00 ** | 100.00 ** |
| Min (%) | 37.43 | 21.11 * | 60.88 | 63.55 | 70.58 | 76.74 ** |
| RMSE | 53.94 | 77.57 ** | 69.46 | 51.28 | 17.21 * | 18.86 |

* Minimum value, ** Maximum value.

The results of the comparison analyses of the daylight illuminance prediction accuracy with the clearness index are shown in Figure 18. Regression analysis of the daylight illuminance prediction accuracy data and the clear index data showed that the coefficient of determination ($R^2$) value was 0.1004. As a regression analysis results, there is no correlation between the daylight illuminance prediction accuracy data and the clear index data.

Figure 19 shows the daily average prediction accuracy of the daylight illuminance and the daily clearness index for the studied points. The data for which the measured daylight illuminance exceeded the target illuminance were excluded from the calculation of the prediction accuracy. For P1 and P2 near the window, the daylight illuminance exceeded the target illuminance. The daylight illuminance did not exceed the target illuminance for 5–6 d, and the prediction accuracy is shown in the form of a dotted line and not a continuous line in Figure 19a,b.

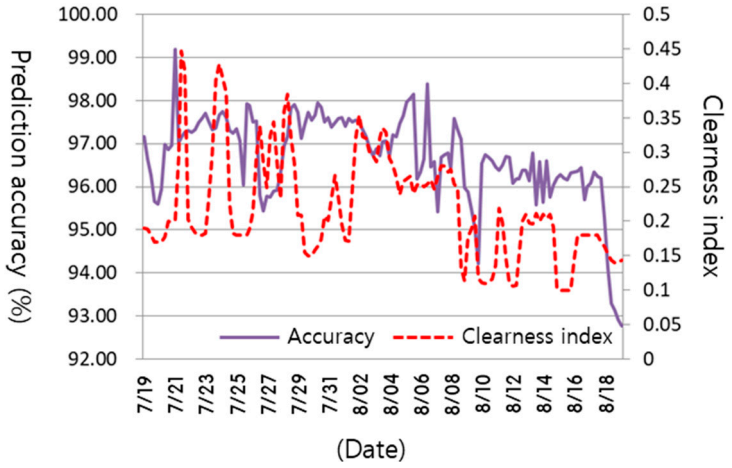


**Figure 18.** Variations of the prediction accuracies for the daylight illuminance on the workplane and clearness index.

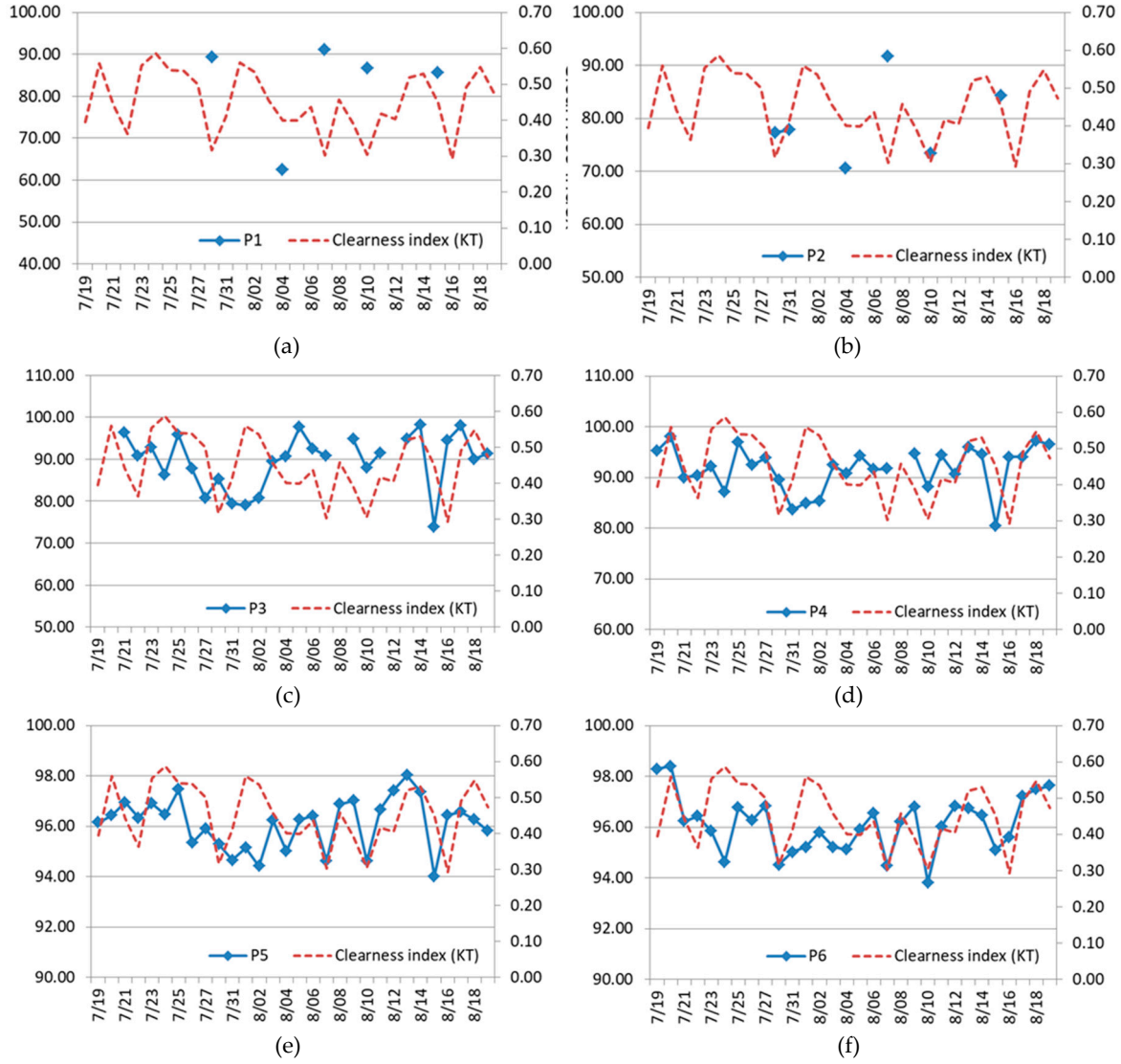


**Figure 19.** Daily average daylight illuminance on the workplane prediction accuracy and daily clearness index for points (**a**) P1, (**b**) P2, (**c**) P3, (**d**) P4, (**e**) P5, and (**f**) P6.

Table 6 shows the prediction accuracy of the daylight illuminance for points P1–P6 according to the sky conditions. For partly cloudy skies, P1 and P2 were excluded from the accuracy calculation because the daylight illuminances of P1 and P2 during daylight exceeded the target illuminance. The prediction accuracy of P1, P2, P5, and P6, did not exhibit a particular tendency regarding the sky conditions and target illuminance accuracy. Conversely, P3 and P5 tended to be more accurate as the amount of clouds increased.

**Table 6.** Prediction accuracy of the daylight illuminance on the workplane for points P1–P6 according to the sky conditions.

| Sky Condition | P1 (%) | P2 (%) | P3 (%) | P4 (%) | P5 (%) | P6 (%) |
|---|---|---|---|---|---|---|
| Clear | 85.49 | 81.16 | 62.93 * | 69.85 | 95.32 ** | 93.82 |
| Partly cloudy | - | - | 76.84 * | 84.92 | 96.34 ** | 96.26 |
| Overcast | 89.06 | 84.30 * | 90.37 | 91.12 | 95.48 | 95.81 ** |

* Minimum value, ** Maximum value.

### 3.3. Evaluation of Energy Savings

After sunset, all six luminaires (LED, 40 W) installed in the test-bed were turned on at 100%, and the workplane illuminances were measured. As a result, the average workplane illuminance was measured as approximately 1,000 lx. Because the target illuminance was set to 500 lx, the luminaires were dimmed such that the average workplane illuminance was 500 lx. When the average workplane illuminance was 500 lx, the power consumption of the all luminaires was measured as 104 W (936 Wh per day, for 9 h, between 09:00–18:00). Therefore, the lighting energy savings were analyzed on the basis of 104 W (936 Wh per day). Figure 20 shows the graph of the lighting energy-savings ratio.

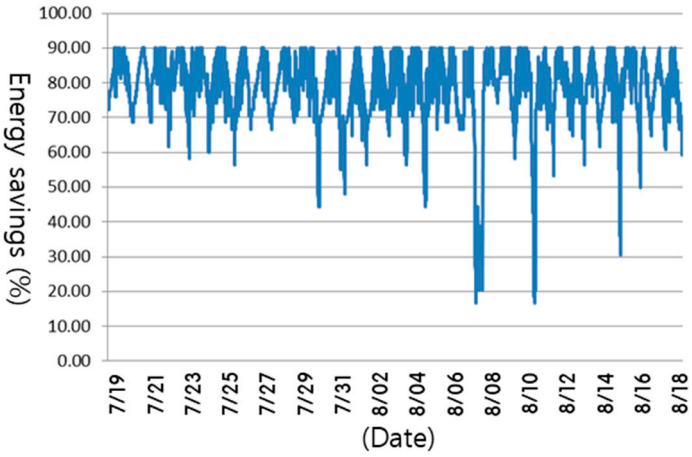


**Figure 20.** Daily results for the lighting energy-savings ratio.

The average daily lighting power consumption was 202.2 Wh (22.5 W), and the average daily lighting energy-savings ratio was 78.4%. The evaluation in this study was conducted during the summer with an abundance of solar radiation, and the lighting energy savings may be lower in other seasons. The maximum lighting energy saving was determined to be 90.1%. This is because the luminaires consumed standby power (approximately 9.6 W) even when turned off. If a low-standby power luminaire is used, the maximum lighting energy savings ratio can be increased from 91.1% to nearly 100%. The minimum amount of lighting energy savings was 16.6% with rainy or overcast skies.

Figure 21 shows the comparison analyses of the lighting energy-savings ratio and clearness index. Regression analysis of the lighting energy-savings ratio data and clearness index data showed that the coefficient of determination ($R^2$) value was 0.2812. As a regression analysis results, there is no correlation between the lighting energy-savings ratio data and clearness index data. Table 7 shows the lighting power consumption and lighting energy-savings ratio according to the sky conditions.

The average amount of lighting energy savings was the largest in the clear sky condition (approximately 89.7%), which was rich in daylight, and the smallest in the overcast sky condition (approximately 73.8%). There was no significant difference in the average lighting energy savings between the clear sky condition and the partly cloudy sky condition.

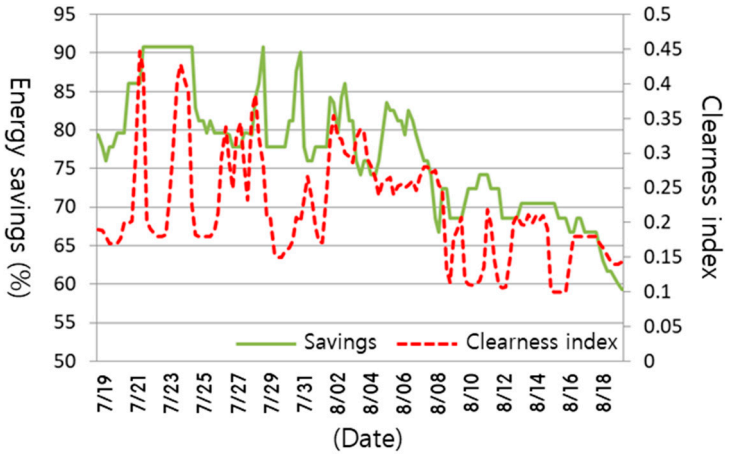


**Figure 21.** Variations of the the lighting energy-savings ratio and clearness index.

**Table 7.** Lighting power consumption and lighting energy-savings ratio according to the sky conditions.

| Sky Condition | Average Power Consumption (W) | Daily Power Consumption (Wh) | Savings (%) |
|---|---|---|---|
| Clear | 10.75 | 96.78 | 89.67 |
| Partly cloudy | 15.54 | 139.83 | 85.08 |
| Overcast | 27.30 | 245.73 | 73.78 |

## 4. Conclusions

We proposed an advanced commissioning and a dimming control algorithm considering the influences of illuminance by distant luminaires for the DRDS. Additionally, we evaluated the daylight illuminance prediction accuracy, the target illuminance achieved by maintaining the accuracy, and the lighting energy savings of the proposed method.

The average daylight illuminance prediction accuracy was 95.5% (SD 3.4%). The maximum accuracy was 100%, and the minimum accuracy was 71.46%. The accuracies for P5 and P6 placed near the door were higher than those for P1 and P2.

As a result of the target illuminance accuracy analyses, the average target illuminance accuracy was 96.9% (SD 2.2%). The maximum and minimum accuracies were maintained at increased levels of 100% and 73.9%, respectively.

The daylight illuminance prediction accuracy was 95.5% (SD 3.4%), and the maximum and minimum accuracies were 100% and 71.5%, respectively.

As a result of the lighting energy savings, the daily average lighting power consumption was 202.2 Wh (22.5 W). The average amount of lighting energy savings was 78.4%, and the maximum amount of lighting energy savings was 90.1%. This is because the luminaires consumed standby power (approximately 9.6 W) even when turned off. The minimum lighting energy-savings ratio was 10.3%. This result is different from the general office luminous environment as a result of the experiment on the test bed without shade on the window. When a shade is installed on a window to reduce the glare caused by daylight, the amount of incident daylight is reduced. For this reason, the amount of light energy savings can be less than the amount reported in this study.

The dimming step of the luminaire installed on the full-scale test-bed was 20 steps. If a luminaire with better dimming performance is used, the lighting energy savings and the target illuminance accuracy can be improved. In future studies, to improve the target illuminance accuracy, we will develop an algorithm that increases the accuracy of the daylight illuminance prediction using photo

sensors. Through the development of this advanced algorithm, we intend to maximize lighting energy savings and provide a comfortable luminous environment.

**Author Contributions:** Conceptualization, I.-T.K. and Y.-S.K.; Methodology, A.C.; Software, I.-T.K. and H.N.; Validation, I.-T.K., Y.-S.K. and T.H.; Formal Analysis, I.-T.K., Y.-S.K. and A.C.; Investigation, Y.-S.K. and M.C.; Resources, H.N.; Data Curation, M.C.; Writing-Original Draft Preparation, I.-T.K.; Writing-Review & Editing, T.H.; Visualization, H.N. and T.H.; Supervision, T.H.; Project Administration, A.C. and T.H.; Funding Acquisition, Y.-S.K. and T.H.

**Funding:** This work was supported by the Korea Institute of Energy Technology Evaluation and Planning (KETEP) and the Ministry of Trade, Industry & Energy (MOTIE) of the Republic of Korea (No. 20182010600110). This work was supported by the Korea Institute of Energy Technology Evaluation and Planning (KETEP) and the Ministry of Trade, Industry & Energy (MOTIE) of the Republic of Korea (No. 20184010201650).

**Acknowledgments:** This work was supported by the Korea Institute of Energy Technology Evaluation and Planning (KETEP) and the Ministry of Trade, Industry & Energy (MOTIE) of the Republic of Korea (No. 20182010600110). This work was supported by the Korea Institute of Energy Technology Evaluation and Planning (KETEP) and the Ministry of Trade, Industry & Energy (MOTIE) of the Republic of Korea (No. 20184010201650).

**Conflicts of Interest:** The authors declare no conflict of interest.

## Nomenclature

| | |
|---|---|
| DRDS | Daylight responsive dimming system |
| $ET_j$ | Final work plane illuminance at the position directly under the luminaire (j) |
| $E_j$ | Work plane illuminance at the position directly under the luminaire (j) |
| $E_{ij}$ | Work plane illuminance at the position directly under the luminaire (j) by luminaire (i) |
| $ED_j$ | Daylight illuminance at the position directly under the luminaire (j) |
| $n$ | Number of luminaires in the room |
| $ER_j$ | Required illuminance at the position directly under the luminaire (j) |
| $g(L_j)$ | Regression equation of work plane illuminance at the position directly under the luminaire (j) according to the dimming level of the luminaire (j) |
| $IE_{ij}$ | Proportion of work plane illuminance at the position directly under the luminaire (i) and work plane illuminance at the position directly under the luminaire (j) by luminaire (i) |

## References

1. Ministry of Land. *Infrastructure and Transport, to Cope with Climate Change Zero Energy Building Promotion Plan*; National Building Policy Committee Reporting; Ministry of Land: Sejong City, Korea, 2016.
2. Son, W.D. *Commercialization of Green Building Remodelling Project for Private Buildings, Building Energy Seminar*; Seoul Energy Dream Center: Seoul, Korea, 2015.
3. Costanzo, V.; Evola, G.; Marletta, L.; Pistone Nascone, F. Application of Climate Based Daylight Modelling to the Refurbishment of a School Building in Sicily. *Sustainability* **2018**, *10*, 2653. [CrossRef]
4. Piderit Moreno, M.B.; Labarca, C.Y. Methodology for assessing daylighting design strategies in classroom with a climate-based method. *Sustainability* **2015**, *7*, 880–897. [CrossRef]
5. Kwon, C.; Lee, K. Integrated Daylighting Design by Combining Passive Method with DaySim in a Classroom. *Energies* **2018**, *11*, 3168. [CrossRef]
6. Acosta, I.; Campano, M.Á.; Domínguez-Amarillo, S.; Muñoz, C. Dynamic Daylight Metrics for Electricity Savings in Offices: Window Size and Climate Smart Lighting Management. *Energies* **2018**, *11*, 3143. [CrossRef]
7. Oh, M.; Park, J.; Roh, S.; Lee, C. Deducing the Optimal Control Method for Electrochromic Triple Glazing through an Integrated Evaluation of Building Energy and Daylight Performance. *Energies* **2018**, *11*, 2205. [CrossRef]
8. Lee, K.S.; Han, K.J.; Lee, J.W. Feasibility study on parametric optimization of daylighting in building shading design. *Sustainability* **2016**, *8*, 1220. [CrossRef]
9. Guan, Y.; Yan, Y. Daylighting Design in classroom based on yearly-graphic analysis. *Sustainability* **2016**, *8*, 604. [CrossRef]
10. Mohelníková, J.; Míček, D.; Floreková, S.; Selucká, A.; Dvořák, M. Analysis of Daylight Control in a Chateau Interior. *Build* **2018**, *8*, 68. [CrossRef]

11. Moazzeni, M.H.; Ghiabaklou, Z. Investigating the influence of light shelf geometry parameters on daylight performance and visual comfort, a case study of educational space in Tehran, Iran. *Build* **2016**, *6*, 26. [CrossRef]
12. Kaminska, A.; Ożadowicz, A. Lighting Control Including Daylight and Energy Efficiency Improvements Analysis. *Energies* **2018**, *11*, 2166. [CrossRef]
13. Vu, N.H.; Shin, S. Flat Optical Fiber Daylighting System with Lateral Displacement Sun-Tracking Mechanism for Indoor Lighting. *Energies* **2017**, *10*, 1679. [CrossRef]
14. Lee, K.S.; Han, K.J.; Lee, J.W. The Impact of Shading Type and Azimuth Orientation on the Daylighting in a Classroom–Focusing on Effectiveness of Façade Shading, Comparing the Results of DA and UDI. *Energies* **2017**, *10*, 635. [CrossRef]
15. Kim, S.H.; Kim, I.T.; Choi, A.S.; Sung, M.K. Evaluation of Optimized PV Power Generation an Electrical Energy Savings from the PV Blind-integrated Daylight Responsive Dimming System Using LED Lighting. *Sol. Energy* **2014**, *107*, 746–757. [CrossRef]
16. Al-Ashwal, N.T.; Budaiwi, I.M. Energy savings due to daylight and artificial lighting integration in office buildings in hot climate. *Int. J. Energy Environ.* **2011**, *2*, 999–1012.
17. Fernandes, L.L.; Lee, E.S.; Ward, G. Lighting energy savings potential of split-pane electrochromic windows controlled for daylighting with visual comfort. *Energy Build.* **2013**, *61*, 8–20. [CrossRef]
18. Caicedo, D.; Pandharipande, A.; Willems, F.M. Daylight-adaptive lighting control using light sensor calibration prior-information. *Energy Build.* **2014**, *73*, 105–114. [CrossRef]
19. Yoo, S.; Kim, J.; Jang, C.Y.; Jeong, H. A sensor-less LED dimming system based on daylight harvesting with BIPV systems. *Opt. Express* **2014**, *22*, A132–A143. [CrossRef]
20. Gentile, N.; Dubois, M.C. Field data and simulations to estimate the role of standby energy use of lighting control systems in individual offices. *Energy Build.* **2017**, *155*, 390–403. [CrossRef]
21. Nagy, Z.; Yong, F.Y.; Frei, M.; Schlueter, A. Occupant centered lighting control for comfort and energy efficient building operation. *Energy Build.* **2015**, *94*, 100–108. [CrossRef]
22. Gentile, N.; Laike, T.; Dubois, M.C. Lighting control systems in individual offices rooms at high latitude: Measurements of electricity savings and occupants' satisfaction. *Sol. Energy* **2016**, *127*, 113–123. [CrossRef]
23. Yun, G.Y.; Kim, H.; Kim, J.T. Effects of occupancy and lighting use patterns on lighting energy consumption. *Energy Build.* **2012**, *46*, 152–158. [CrossRef]
24. Pandharipande, A.; Caicedo, D. Daylight integrated illumination control of LED systems based on enhanced presence sensing. *Energy Build.* **2011**, *43*, 944–950. [CrossRef]
25. Wang, Z.; Tan, Y.K. Illumination control of LED systems based on neural network model and energy optimization algorithm. *Energy Build.* **2013**, *62*, 514–521. [CrossRef]
26. Choi, H.Y.; Hong, S.K.; Choi, A.S.; Sung, M.K. Toward the accuracy of prediction for energy savings potential and system performance using the daylight responsive dimming system. *Energy Build.* **2016**, *133*, 271–280. [CrossRef]
27. Parise, G.; Martirano, L. Daylight impact on energy performance of internal lighting. *IEEE Trans. Ind. Appl.* **2013**, *49*, 242–249. [CrossRef]
28. Ul Haq, M.A.; Hassan, M.Y.; Abdullah, H.; Rahman, H.A.; Abdullah, M.P.; Hussin, F.; Said, D.M. A review on lighting control technologies in commercial buildings, their performance and affecting factors. *Renew. Sustain. Energy Rev.* **2014**, *33*, 268–279. [CrossRef]
29. Park, B.C.; Choi, A.S.; Jeong, J.W.; Lee, E.S. Performance of integrated systems of automated roller shade systems and daylight responsive dimming systems. *Build. Environ.* **2011**, *46*, 747–757. [CrossRef]
30. Li, D.H.; Cheung, G.H.; Cheung, K.L.; Lam, T.N. Determination of vertical daylight illuminance under non-overcast sky conditions. *Build. Environ.* **2010**, *45*, 498–508. [CrossRef]
31. Acosta, I.; Munoz, C.; Campano, M.A.; Navarro, J. Analysis of daylight factors and energy saving allowed by windows under overcast sky conditions. *Renew. Energy* **2015**, *77*, 194–207. [CrossRef]
32. Li, D.H. A review of daylight illuminance determinations and energy implications. *Appl. Energy* **2010**, *87*, 2109–2118. [CrossRef]
33. Korean Standards Association. *KS A3011, KS Recommended Levels of Illumination*; Korea Industrial Standards Certificate: Gyeonggi-do Province, Korea, 1998.
34. Reindl, D.T.; Beckman, W.A.; Duffie, J.A. Diffuse fraction correlations. *Sol. Energy* **1990**, *45*, 1–7. [CrossRef]

35. Park, B.C.; Choi, A.S.; Jeong, J.W.; Lee, E.S. A Preliminary Study on the Performance of Daylight Responsive Dimming Systems with Improved Closed-Loop Control Algorithm. *Leukos* **2011**, *8*, 41–59.
36. Jeong, K.Y.; Choi, A.S.; Sung, M.K. A mock-up study for validation of an improved control algorithm for automated roller shade. *Indoor Built Environ.* **2016**, *25*, 17–28. [CrossRef]

© 2019 by the authors. Licensee MDPI, Basel, Switzerland. This article is an open access article distributed under the terms and conditions of the Creative Commons Attribution (CC BY) license (http://creativecommons.org/licenses/by/4.0/).